Journal of Biomedical Optics

SPIEDigitalLibrary.org/jbo

In-vitro detection of artificial caries on vertical dental cavity walls using infrared photothermal radiometry and modulated luminescence

Jungho Kim
Andreas Mandelis
Stephen H. Abrams
Jaclyn T. Vu
Bennett T. Amaechi

In-vitro detection of artificial caries on vertical dental cavity walls using infrared photothermal radiometry and modulated luminescence

Jungho Kim,[a] Andreas Mandelis,[a,b] Stephen H. Abrams,[b] Jaclyn T. Vu,[c] and Bennett T. Amaechi[c]
[a]University of Toronto, Center for Advanced Diffusion-Wave Technologies, Department of Mechanical and Industrial Engineering, 5 King's College Road, Toronto, Ontario M5S 3G8, Canada
[b]Quantum Dental Technologies Inc., 748 Briar Hill Avenue, Toronto, Ontario M6B 1L3, Canada
[c]University of Texas Health Science Center at San Antonio, Department of Comprehensive Dentistry, 7703 Floyd Curl Drive, San Antonio, Texas 78229-3900

Abstract. The main objective of the study was to investigate the ability of frequency-domain photothermal radiometry (PTR) and modulated luminescence (LUM) to detect secondary caries lesions on the walls of restorations (wall lesions). Changes in experimental PTR-LUM signals due to sequential demineralization on entire vertical walls of sectioned tooth samples were investigated. In addition, transverse micro-radiography (TMR) analysis (used as a gold standard) was conducted to measure the degree of demineralization that occurred in each sample. Statistical correlation between TMR results and PTR-LUM signals was determined using Pearson's correlation coefficient. LUM signals were found to be dominated by the scattered component of the incident laser beam. The more clinically relevant cases of localized demineralization and remineralization on vertical walls were also investigated to examine whether PTR-LUM signals are sensitive to demineralization and remineralization of much smaller areas. The overall results demonstrated that PTR-LUM is sensitive to progressive demineralization and remineralization on vertical walls of sectioned tooth samples. © *2012 Society of Photo-Optical Instrumentation Engineers (SPIE).* [DOI: 10.1117/1.JBO.17.12.127001]

Keywords: caries; demineralization; luminescence; photothermal radiometry; remineralization; secondary caries; wall lesions.

Paper 12485 received Jul. 27, 2012; revised manuscript received Oct. 20, 2012; accepted for publication Oct. 30, 2012; published online Dec. 3, 2012.

1 Introduction

Secondary caries is the carious lesion developed on the cavity walls beneath and around dental restorations and may or may not be clinically visible around the margins of the restoration.[1,2] Hence, secondary caries can be categorized into wall and surface (outer) lesions.[3–5] The wall lesion develops on the interfacial wall of the tooth and the restoration, and the outer lesion occurs on the outside surface around the margins of the restoration. While the outer lesion is caused by plaque accumulation at the restoration margins, the wall lesion is considered to be caused by the presence of a gap at the tooth-restoration interface, which allows the formation of a biofilm on the cavity walls due to seepage of saliva between the cavity wall and the restoration.[6–10] Thus wall lesions occur at subsurface regions that are not clinically visible with traditional visual examination and are only detectable by radiography at an advanced stage.[11–16] Therefore, the development of a novel method to detect wall lesions is considered an advancement in caries detection and diagnosis.

The main objective of this study was to investigate the ability of the combined technique of photothermal radiometry (PTR) and modulated luminescence (LUM) to detect and monitor the development of wall lesions. In our previous studies we demonstrated the ability of PTR-LUM to detect pit and fissure caries on the occlusal surface of teeth as well as root surface caries.[17–19] For most of the studies, PTR-LUM signals were measured directly on the demineralized surface. The same method could be used to investigate the outer lesions around restorations. However, for the case of wall lesions, PTR-LUM signals had to be measured on the surface adjacent, and perpendicular, to the demineralized surface. Therefore, a new experimental method had to be developed to study the detection of wall lesions; lesions along the entire wall or lesions on a small area beneath the tooth surface.

The first step of the study was to assess the PTR-LUM system by investigating the signals collected from a vertically sectioned half-tooth sample placed against different materials: composite resin block, glass, and mirror. PTR-LUM signals were also collected while changing the interfacial gap size between the half-tooth sample and the composite resin block. From this preliminary study we could demonstrate the capability of the PTR-LUM system to sense the different boundary conditions introduced by various materials and interfacial gap sizes.

The next step was to demonstrate that PTR-LUM is sensitive to relatively large size of wall lesions that were artificially developed in a laboratory setting. PTR-LUM signals were collected upon sequential demineralization on the entire vertical wall of sectioned tooth samples. TMR analysis (considered as a gold standard) was conducted to measure the actual physical changes of the tooth samples resulted from demineralization process and

Address all correspondence to: Andreas Mandelis, University of Toronto, Center for Advanced Diffusion-Wave Technologies, Department of Mechanical and Industrial Engineering, 5 King's College Road, Toronto, Ontario M5S 3G8, Canada. Tel: 1-416-978-5106; Fax: 1-416-266-7867; E-mail: mandelis@mie.utoronto.ca

correlate this anatomical result to PTR-LUM measurements, i.e., to see whether the changes in PTR-LUM signals are due to demineralization effects or some other reasons.

Subsequently, the more clinically relevant case of localized demineralization and remineralization on the vertical wall was investigated. PTR was used to investigate optothermal characteristics of the treated tooth samples, while LUM was simultaneously used to investigate optical propagation and photon diffusion (scattering) characteristics in the samples. Our main hypothesis was that demineralization and remineralization processes along the vertical wall would cause changes in the optical and thermal properties of the treated area, thereby introducing a new boundary condition which affects both thermal- and optical-wave distributions in the volume of the turbid dental medium, resulting in changes of both PTR and LUM signals.

The successful development of this methodology is of interest to the dental profession. Its successful clinical implementation will provide a minimally invasive technique for lesion detection at an early stage in the caries process and prevent unnecessary removal and replacement of existing restorations as a screening method for secondary caries, which will minimize cost and time. Moreover, if secondary caries can be detected at an early stage, application of an appropriate remineralization therapy will restore the lesion site to its original healthy condition, which will result in long-term dental health and economic benefits.

2 Materials and Methods

2.1 *Experimental Setup*

Figure 1 shows the schematic diagram of the experimental setup for combined PTR and LUM monitoring. A semiconductor laser diode with wavelength 660 nm and maximum power 130 mW was used as a radiation source (Opnext, HL6545 MG). A laser diode controller (Thorlabs, LDC202B) triggered by a software lock-in amplifier (National Instruments, NI6221) modulated the laser current. The modulated laser beam was focused on the surface of a tooth sample with the aid of lenses (Thorlabs, LMR1) as indicated in Fig. 1. The modulated PTR response of the tooth sample was focused by two off-axis paraboloidal mirrors and was collected by the HgCdZnTe [mercury cadmium telluride (MCT)] detector (VIGO, PVI-2TE-5) as indicated with arrows in Fig. 1. The HgCdZnTe detector was optimized for the maximum performance at the optimal wavelength of 5 μm. This is in the mid-infrared spectral range. The LUM response was focused onto a photodetector (Thorlabs, PDA36A). A cut-on optical colored filter (cut-on wavelength 715 nm, Edmund Optics) was placed in front of the photodetector to block unwanted laser light reflected or back-scattered by the tooth. Collected PTR-LUM signals were digitized and stored using a software lock-in amplifier (National Instruments, NI6221) and Labview software.

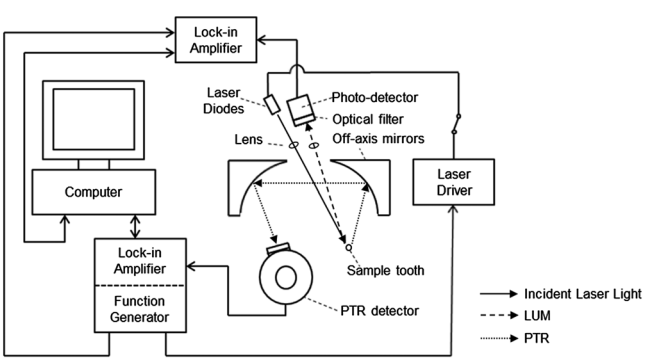

Fig. 1 Schematic diagram of the experimental setup for combined PTR and LUM: a solid arrow indicates the direction of the incident laser light focused on to the sample tooth, a coarse dashed arrow indicates the direction of the LUM signal collected with the photodetector; and fine dashed arrows indicate the direction of the PTR signal collected with the MCT detector.

2.2 *Sample Preparation*

2.2.1 *Materials adjacent to a vertically sectioned tooth sample*

An extracted human tooth was vertically sectioned in half using a diamond-tipped cutter. One of the two half teeth was mounted on a Lego block with the aid of plastic epoxy. Using the heavily filled large particle composite restoration material Heliomolar (IvoclarVivadent) shade A3, a small structure of a composite restoration was built on a separate Lego block against the sectioned vertical wall of the half-tooth sample as shown in Fig. 2. The composite restoration material was packed and light-cured every 2 mm of thickness according to the manufacturer's instructions. The prepared sample was stored in a humid container to prevent it from dehydration that can cause structural damage. Structures with glass and mirror were also prepared to test the effects of transmitted and reflected laser radiation through the vertical surface on the PTR and LUM signals.

2.2.2 *Development of artificial wall lesions—Case 1: Demineralization of the entire sectioned tooth wall*

Several extracted human teeth, free of cracks, stains, brown spots, or white spots were collected. They were vertically sectioned in half, and each half tooth was mounted on a Lego block using the same technique mentioned in Sec. 2.2.1. Four samples were prepared in total and each sample was numbered from 1 to 4. The prepared samples were stored in a humid container to prevent dehydration-induced damage such as micro-cracks. The

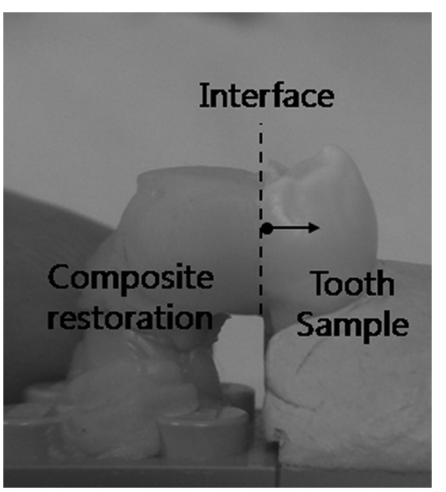

Fig. 2 A vertically sectioned half-tooth sample mounted on a Lego block with a composite restoration block built on a Lego block against the vertically sectioned wall of the tooth sample. PTR-LUM scans commenced near the interfacial edge indicated as a dot and moved up to 2 mm away from the edge in the direction of an arrow.

samples were demineralized using a standard acidified gel [0.1 M lactic acid ($C_3H_6O_3$) gelled to a thick consistency with 14% hydroxyethyl cellulose (HEC) and adjusted to pH 4.5 with the addition of 0.1 M NaOH] in order to develop artificial wall lesions on the entire cut surface of the vertical walls of the tooth samples. The tooth samples were mounted on a fixed support in the treatment cell with the sectioned flat surface facing downward on to the demineralization gel. Initially the tooth samples did not contact the gel, then the gel surface was slightly elevated until it touched the entire surfaces of the sectioned walls. The gel was applied only on the sectioned surface while leaving all other surfaces intact. It remained in contact with the flat tooth surface by means of surface tension. Line and frequency PTR-LUM scans were conducted before demineralization (control) and after 1, 2, 3, 5, 7, 10, and 14 days of demineralization. The samples were cleaned with running tap water and naturally dried inside a humid container for at least 2 h in order to remove excessive water. Therefore, there remained a residual humidity only due to ambient conditions to which the PTR signals have little or no sensitivity. The samples continued to be demineralized after each scanning examination.

2.2.3 *Development of artificial wall lesions—Case 2: Localized demineralization and remineralization*

Sample preparation and demineralization procedures were the same as for the entire wall demineralization in Sec. 2.2.2; however, in this case, only localized artificial wall lesions were created by covering the sectioned surface with an adhesive tape [colored Unplasticised PolyVinyl Chloride (UPVC) tape, 3 M] except for an exposed small fraction of the surface of approximately 1 mm diameter, where localized demineralization occurred upon exposure to treatment solutions. The samples were scanned before demineralization (control) and after 1, 2, 3, 5, 7, 10, and 14 days of demineralization with PTR-LUM line and frequency scans. The tape was removed after each stage of lesion development, and the sample was cleaned with running tap water in order to remove the demineralization gel and any residual adhesives. The samples then continued to be demineralized in the same manner after conducting PTR-LUM scans. The developed localized lesions were then subjected to 6 weeks of remineralization using artificial saliva that consisted of 1.5 mM $Ca(NO_3)_2$, 0.9 mM KH_2PO_4, 130 mM KCl, and 20 mM cacodylic acid, pH adjusted to 7.0 using KOH. During the remineralization period, the artificial saliva was replaced every 3 days, while PTR-LUM measurements were made on a weekly basis. The first 4 weeks of remineralization were conducted with only artificial saliva; however, during the last 2 weeks, the remineralization process was accelerated with 1500 ppm fluoride solution using a pH cycling model. The remineralization process was changed from continuous remineralization to pH cycling when high fluoride solution was being used in order to accelerate the remineralization process. The pH cycling model with the demineralization phase keeps the pores on the outer surface of the lesion open to enable uptake of remineralizing elements (fluoride, calcium, and phosphate) into the inner layer of the lesion and cause more homogenous and accelerated remineralization of the lesion layers. Without the demineralization phase, the high fluoride would cause rapid remineralization of the surface layer, blocking the pores on the surface layer and limiting the uptake of the remineralizing elements into the inner layer and slowing down the remineralization process. The pH (demineralization and remineralization) cycle mimicked the natural pH cycle in the mouth, i.e., during and after eating, teeth undergo demineralization; subsequently, saliva aids in remineralizing the demineralized surfaces. The additional remineralization solution (1500 ppm NaF) simulated the use of a fluoride toothpaste or mouth rinse to enhance remineralization. The daily treatment cycle consisted of two 5-min remineralizations in fluoride solution, two 2-min demineralizations in acidic solution (2.2 mM KH_2PO_4, 50 mM acetic acid, 2.2 mM of 1 M $CaCl_2$, and 0.5 ppm fluoride, pH 4.5 adjusted by KOH), three 3-h artificial saliva treatments, and a 15-h overnight storage in artificial saliva.

2.3 *PTR-LUM Scanning Procedures*

There were two types of PTR-LUM scans conducted throughout the study: a frequency scan and a line scan. The frequency scan was performed at a fixed position on the tooth surface to examine the frequency dependence of PTR and LUM signals from 2 to 200 Hz. Measurements were made at one frequency starting from 2 Hz, and the frequency was automatically increased using Labview software. Four frequency values were used for most of the experiments throughout the study: 2, 6, 15, and 200 Hz. Four frequencies were used to save the measurement time and thereby prevent the tooth samples from over-dehydration. A preliminary pilot study showed that four frequencies are sufficient to define the frequency dependence of the signal. There was at least a 15-s delay between measurements at each frequency in order to allow the signals to stabilize upon frequency change. Changing the frequency allowed one to examine various depths beneath the tooth surface.[17–19]

Line scans were performed to measure PTR and LUM signals along a spatial coordinate on the tooth surface at a fixed frequency and they were conducted along a line on the tooth sample starting from the sectioned edge and moving away from the tooth-restoration interface. The micrometer stage where the tooth sample was placed was adjusted to move to the next measurement position. After each change of measurement position, there was a 15-s delay time for signal stabilization.

2.3.1 *Materials adjacent to a vertically sectioned tooth sample*

Various materials, including the composite restoration block, the glass, and the mirror, were placed against the sectioned vertical surface of the half-tooth sample, and line scans were conducted on the side surface of the tooth sample perpendicular to the sectioned vertical surface touching the adjacent materials. Glass and mirror interfaces were extremely helpful in assessing the effects of scattered and vertical interface-propagated optical-wave distributions in the volume of the turbid dental medium, which resulted in changes of both PTR and LUM signals. Scans commenced near the interfacial edge as indicated with a dot in Fig. 2 and moved up to 2 mm away from the edge in the direction of an arrow in the same figure. Another set of scans was conducted where a half-tooth sample was initially in contact with a composite restoration block, and the interfacial gap was gradually increased while the change in PTR-LUM signals was recorded at, and perpendicularly to, the interfacial edge on the side surface of the tooth sample (indicated with a dot in Fig. 2). The composite restoration block built on a Lego block was placed on a uni-axial micrometer stage. Controlled movement of the composite restoration using the uni-axial

micrometer stage made it possible to set a desired value of gap size between the restoration and the vertical wall of the tooth.

2.3.2 *Development of artificial wall lesions—Case 1: demineralization of the entire sectioned tooth wall*

Both enamel and dentin were affected when demineralizing the entire sectioned surface of the tooth (Fig. 3). Measurement locations were carefully chosen in each sample, since the thickness of enamel varies from enamel to root. Moreover, the thickness of enamel varied between samples. In each case, the measurement line was chosen such that the thickness of the enamel layer was approximately 1 mm. Before a scan, each sample was taken out of the humid container, rinsed thoroughly with running tap water for more than 20 s, and excessive water was removed. Then the sample was placed on a three-axis micrometer sample stage, and the laser was focused onto the sample tooth by adjusting the three-axis micrometer stage. Scanning was done for only 1 h (~20 min for warm up and ~40 min for scanning) to avoid dehydration of the tooth sample.[20] Line and frequency scans were conducted at several stages of demineralization: before demineralization and after 1, 2, 3, 5, 7, 10, and 14 days demineralization. The composite restoration was not in place during these scans.

After the last PTR-LUM measurement, following a total of 14 days of demineralization, tooth sections were cut from the zone of the line scan. The sections were microradiographed and analyzed to determine the degree of demineralization for each sample by measuring the mineral loss and lesion depth. Mineral loss and lesion depth values were determined by averaging several scans over the distance of the thin section taken from the center of the demineralized area where PTR-LUM measurements were made. The mineral loss (in vol% μm) was obtained by calculating the difference in volume percent of matter between sound and demineralized tissue integrated over the lesion depth. The mineral content plateau in deeper regions of the enamel section, representative of sound tissue, was pre-set at the 87 vol% level.[21] The lesion depth was determined as the distance from the measured sound enamel surface to the location in the lesion where mineral content was 95% of the sound enamel mineral volume. Statistical analysis was conducted using IBM SPSS Statistics 19 software with significance level (α) pre-chosen at 0.05. Correlation between PTR-LUM signals and TMR results was determined using Pearson's coefficient of correlation.

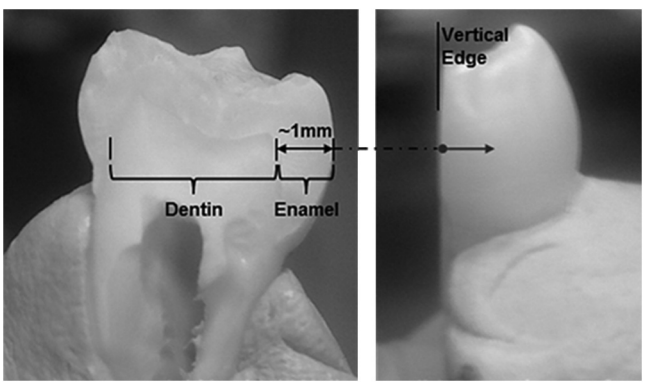

Fig. 3 Vertical tooth wall showing enamel and dentin layer—PTR-LUM scans were conducted on the scanning (side) surface of the tooth where the enamel layer is approximately 1 mm thick. For frequency scans, the laser beam (excitation/probe) was focused at the interfacial edge on the tooth sample, indicated with a dot; and for line scan, the laser beam (excitation/probe) was moved along the line in the direction of the solid arrow shown in the figure.

2.3.3 *Development of artificial wall lesions—Case 2: localized demineralization and remineralization*

PTR-LUM line and frequency scans were conducted after each stage of demineralization using the same protocol as in Sec. 2.3.2. Subsequently, PTR-LUM scans were made with the same samples after 1, 2, 3, 4, and 6 weeks of remineralization. TMR analysis was not performed for this section of study.

3 Results and Discussion

3.1 *Materials Adjacent to a Vertically Sectioned Tooth Sample*

Figure 4 shows results of line scans with the composite resin block, the glass, and the mirror in contact with the sectioned tooth surface. There is a signal strength dependence on the type of material placed against the vertical tooth wall for both PTR and LUM. This is consistent with the effect of vertical surface reflectivity and transmissivity on the overall measured PTR (amplitude and phase) and LUM (amplitude) signals. LUM phases are not shown as they carry no information when they are dominated by scattered light. This was shown to be the case from satellite experiments involving the scattered light from a rough metallic surface. Even under these circumstances, the LUM amplitudes in this study were very useful as they were found to be sensitive to the effects of the changing vertical wall boundary structure on the forward- (exiting) and backward-scattered light from interface materials into the body of the tooth. The shape of the PTR curves is indicative of the dominance of thermal-wave confinement within the gap, as well as between the laser beam incidence location and the vertical wall. The highest LUM signal occurred with the mirror in place (highest reflectivity) and the lowest with no material beside the tooth (zero reflectivity). Figure 4 indicates PTR and LUM sensitivity levels which support signal sensitivity to vertical wall demineralization or breakdown along the margins of the restoration.

Figure 5 shows the PTR and LUM signals obtained at the interfacial edge on the side surface of the sectioned tooth (no demineralization lesion) at a fixed frequency while gradually increasing the gap size. The purpose of these measurements was to assess the effect of gap size on the PTR and LUM signals due to optical and thermal-wave confinement. PTR signals were obtained at 2 Hz and LUM signals at 20 Hz so as to optimize signal-to-noise ratio (SNR) for each channel. Measurements were taken at 100-μm increments of gap size from 0 to 1000 μm and at 500-μm increments from 1000 to 5000 μm. PTR plots show that after ~100 μm only small changes due to thermal-wave confinement effects appear, and they indicate that gaps larger than 100 to 200 μm behave as semi-infinite. Clinically acceptable gap sizes are in the range of 119 to 160 μm.[22,23] Therefore, our PTR and LUM measurements are expected to be sensitive to the gap size in clinical practice. The PTR phase shows sensitivity within error to the presence of restorations up to ~500-μm gap size. However, LUM amplitude plots show that further increases in gap size clearly affect the signals up to the relatively large gap size of 4000 μm. These PTR

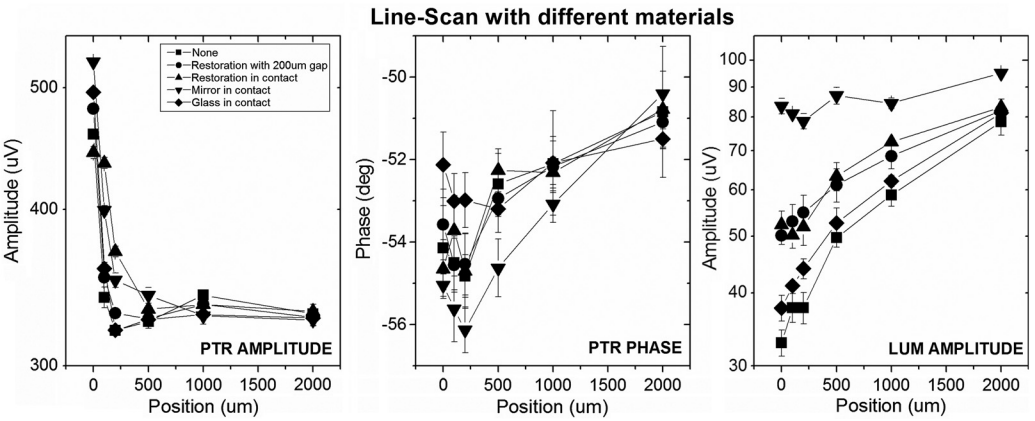

Fig. 4 PTR-LUM line scan results collected on the side surface of the tooth with materials of different optical properties placed adjacent to the vertical wall of the half-tooth sample. Zero position on *x*-axis represents the interfacial edge of the tooth. There was no lesion on the vertical wall.

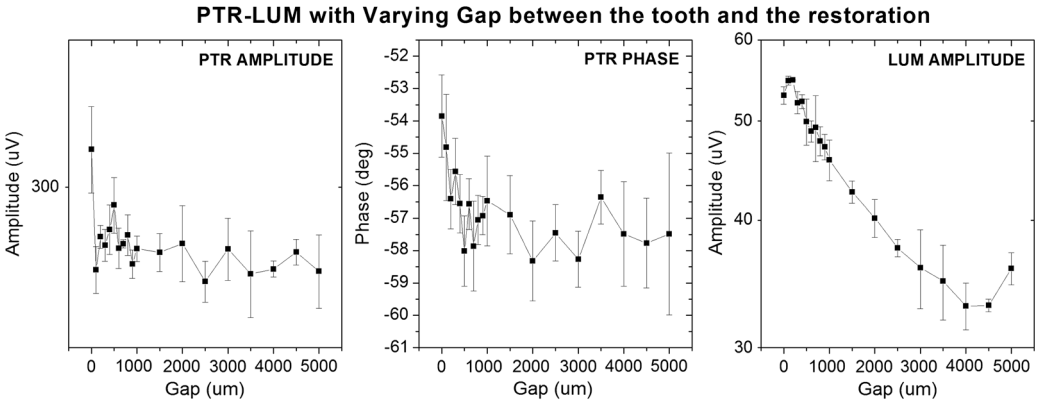

Fig. 5 PTR-LUM signals collected at the interfacial edge on the side surface of the tooth with different gap sizes between the tooth and the composite restoration: PTR signals were obtained at 2 Hz; LUM signals were obtained at 20 Hz.

observations are consistent with the size of the thermal diffusion length, μ_{th}, in air. Using the equation

$$\mu_{th}(f) = \sqrt{\frac{\alpha}{\pi f}}, \tag{1}$$

where α is the thermal diffusivity of the periodically heated medium ($\alpha_{\text{air}} = 0.19$ cm^2/s) and f is the modulation frequency, it is found that $\mu_{\text{th}}(2\text{ Hz}) = 0.17$ cm. The presence of a gap of less than 0.17 cm results in thermal-wave confinement in the inter-gap region yielding larger amplitudes and smaller phase lags than the semi-infinite gap. The LUM results are also consistent with a back-reflection mechanism from the material surface of the far (vertical) wall of the gap. Highly reflective surfaces (mirror) contribute the largest LUM amplitude, Fig. 4. A restoration with a rough surface contributes slightly more back-scattered signal when in contact with the vertical wall than at 200-μm separation. With contacting glass there is little reflection from the front surface due to refractive index mismatch, as most light exiting the vertical wall of the sectioned tooth is transmitted beyond the surface of the glass. Finally, semi-infinite gap contributes no reflected light (lowest LUM amplitude). In summary, these results indicate that the presence of a gap does affect the optical and thermal-wave signals and therefore the PTR and LUM signals are sensitive to a combination of the presence of gap and vertical wall lesions.

3.2 *Development of Artificial Wall Lesions—Case 1: Demineralization of the Entire Sectioned Tooth Wall*

Figure 6 shows the line scan results obtained after each period of demineralization on entire vertical sectioned wall with one representative tooth sample. The PTR amplitude plots show a decrease upon demineralization, although the trend is not monotonic. LUM signals also decrease with demineralization. The non-monotonic temporal behavior of the PTR signal line scans is very interesting as it is consistent with other PTR observations in our laboratory involving demineralization of intact (whole) dental enamel surfaces using the same gel. It appears that the state of demineralization of the vertical wall follows similar trends as intact outer dental enamel surfaces and the PTR signal is controlled by wall demineralization processes, as expected. In PTR amplitude plots in Fig. 6 note the thermal-wave interference pattern between laser beam position and vertical wall for distances < 250 μm in the untreated and treated sample. Before demineralization, the PTR amplitudes at locations adjacent to the vertical wall edge rapidly increased as expected from a thermal standing wave formed due to coherent thermal-wave accumulation at the wall interfering (i.e., superposed) with the forward diffusing wave; however, this phenomenon started to disappear with more days of demineralization as the sharp vertical enamel—air interface gave way to a

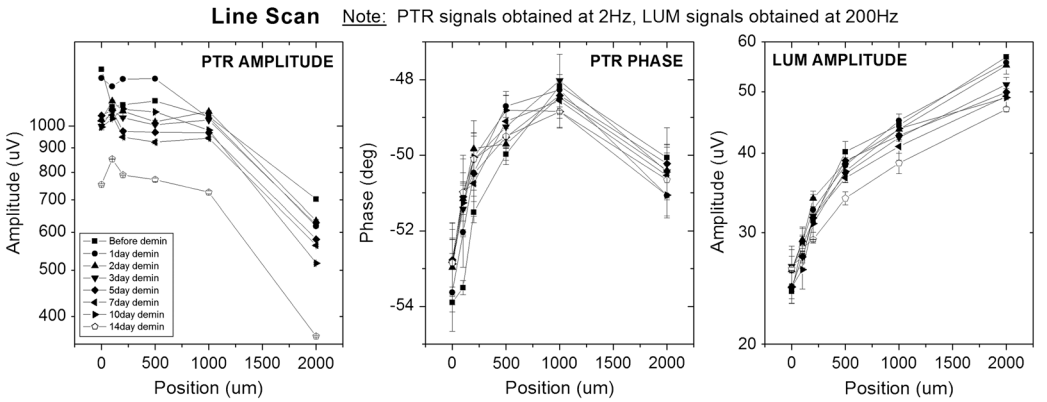

Fig. 6 PTR-LUM line scan results obtained after each period of demineralization of the entire sectioned tooth wall.

less structured demineralized layer which scrambled a portion of the superposition between forward diffusing and interface-accumulated thermal waves.

Frequency scans were conducted with the same samples after each demineralization period at two measurement locations on the side (buccal) surface of the tooth: at the edge and 2 mm away from the edge. Figure 7 shows PTR amplitude, PTR phase, and LUM amplitude. PTR amplitudes decrease and PTR phases increase with more days of demineralization. It is important to note that the effect of vertical surface demineralization on the PTR signal can be measured up to 2 mm away from the interface in both amplitudes and phases and up to 15 Hz or more. These distances are too large compared to the relevant thermal diffusion length (a few hundred micrometers). This is consistent with strongly back-scattered light following interaction with the vertical wall which changes the optical field distribution in the bulk of the tooth, thereby contributing to the generation of a photothermal field component at locations away from the interface. At $f > 15$ Hz, the PTR amplitudes become less sensitive to the condition of the vertical wall, as expected from the $f^{1/2}$ dependence of the thermal diffusion length, Eq. (1). However, the phases remarkably retain their sensitivity to the wall condition even for $f \sim 200$ Hz. On the other hand, LUM signal amplitudes are less sensitive to demineralization especially close to the edge.

TMR analysis was performed on each sample to determine the amount of mineral loss and lesion depth after 14 days of demineralization. PTR-LUM signals at two stages of demineralization were used to define one set of independent variables for the calculation of the correlation coefficients: before demineralization and after a total of 14 days of demineralization. For PTR and LUM amplitudes, "14 days demineralization data" were divided by the "before demineralization data" and expressed as percentage signal amplitude change for each sample. For PTR phase, "14 days of demineralization data" were subtracted from the "before demineralization data" to calculate phase shift for each sample. These values were correlated to the values of the mineral loss and lesion depth. There were statistically significant correlations between the PTR amplitude and the mineral loss ($r = 0.941$; $p < 0.05$), and the LUM amplitude and the lesion depth ($r = -0.998$; $p < 0.001$). There was no significant correlation between neither mineral loss and PTR phase/LUM amplitude nor lesion depth and PTR amplitude/phase. A reason could be that the samples experienced a relatively low degree of demineralization. Previous studies conducted in our laboratory used tooth samples demineralized with the same demineralization gel.[19] Their typical mineral loss was more than 1000 vol% μm, and lesion depth was deeper than ~ 60 μm. The mineral loss and lesion depth values of the samples used for this study were 255 ± 41.53 vol% μm and 13.6 ± 3.01 μm, respectively, which indicates that the samples used for this study experienced a much lower degree of demineralization. It was expected to have a lower degree of demineralization in this study because a small quantity of the demineralization gel was used over a larger area, so the gel gets saturated within a short time by the elements diffusing out of the tooth tissue, and this retards the demineralization process. A higher degree of sample demineralization could have resulted in more drastic changes of PTR-LUM signals and in more statistically significant correlation coefficient values.

3.3 *Development of Artificial Wall Lesions—Case 2: Localized Demineralization and Remineralization*

Figure 8 shows the vertical wall of one representative sample after 1 day of localized demineralization. It is clearly shown that a white spot was created at the top right corner of the vertical wall (indicated with an arrow in the figure) even after 1 day of demineralization, which indicates that demineralization actually occurred and made a physical change to the sample. Figure 9 shows PTR-LUM amplitude and phase signals at several measurement locations (at the edge and at 100 μm, 200 μm, and 2 mm away from the edge) upon progressive demineralization and subsequent remineralization. This figure shows that PTR amplitude decreases upon demineralization. Following remineralization there appears a delayed upward PTR amplitude trend accompanied by a slight downward LUM amplitude trend. The PTR phase exhibits slight increases. It is likely that these trends are due to the changing interface structure at the exposed spot which controls a fraction of the amount of back-reflected and back-scattered light into the tooth bulk. It is clearly seen that even after 1 day of demineralization, the PTR amplitude decreased well beyond the error bar. The timing of signal change is consistent with the fact that a white spot was created even after 1 day of demineralization as shown in Fig. 8. The PTR phase also changed beyond the error bar only after approximately 2 days of demineralization, but the amount of change with respect to the error bar was less than the PTR amplitude. The LUM amplitude changed beyond the error bar after 3 days of demineralization; however, the amount of PTR amplitude change after each demineralization was much larger than that of the LUM amplitude. These results indicate that PTR is more

sensitive to demineralization than LUM. Signal changes due to remineralization of all channels were generally moderate compared to demineralization, presumably due to the slower remineralization rate. The PTR amplitude was sensitive only after 1 week of remineralization. PTR phase changed beyond the error bar after 3 weeks of remineralization. LUM amplitude changed beyond the error bar after 2 weeks of remineralization.

Figures 10 and 11 show line- and frequency-scan results of the same sample, respectively. PTR amplitude signals exhibit a slightly decreasing trend in the first 14 days of progressive demineralization and a reversal, a slightly increasing trend, upon the onset of the subsequent remineralization. Also, the PTR phase keeps increasing during both demineralization and remineralization. LUM amplitude signals exhibit a decreasing pattern at

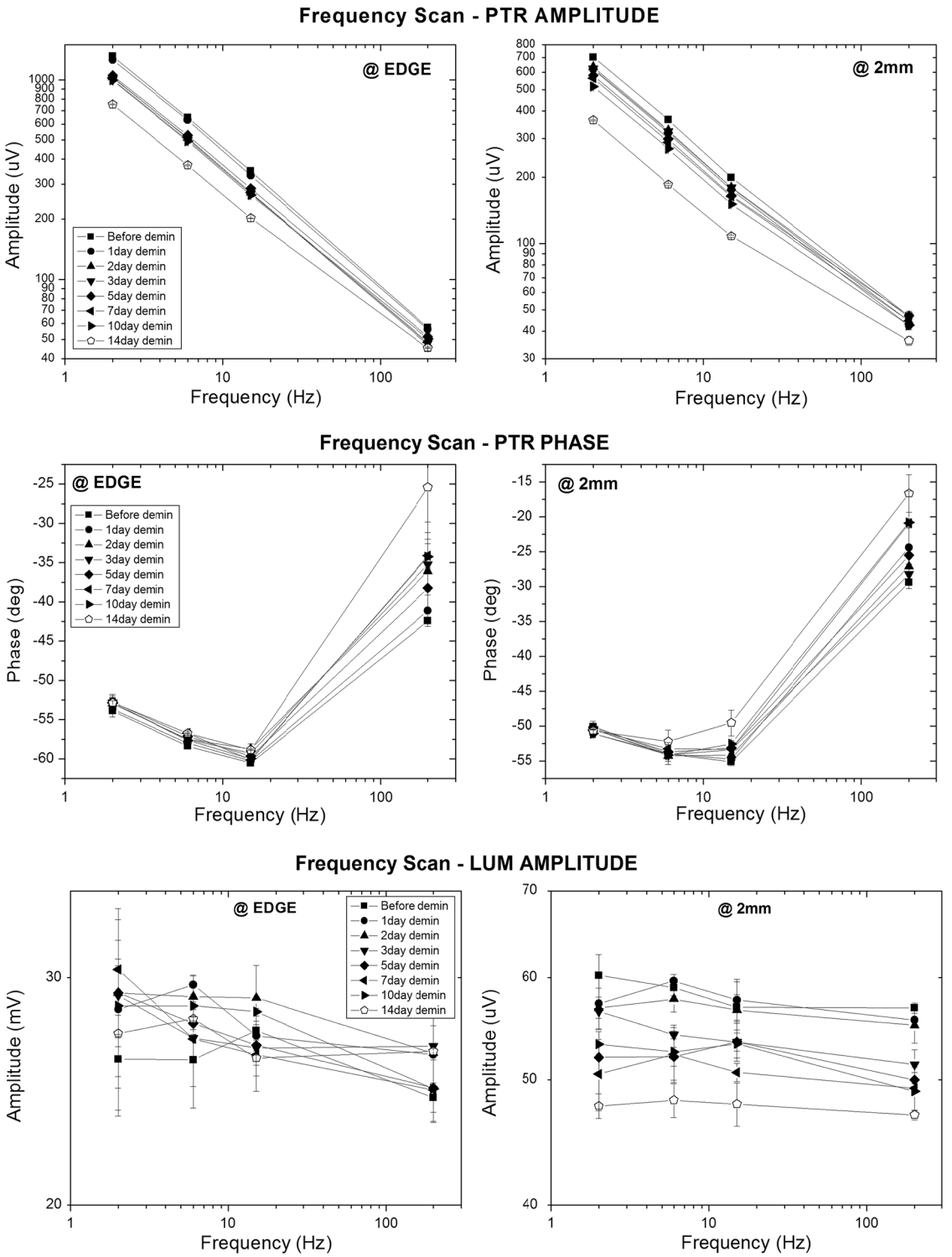

Fig. 7 Frequency scan PTR amplitude, PTR phase, and LUM amplitude obtained after each period of demineralization of the entire sectioned tooth wall, collected at different measurement locations on the side surface of the tooth: at the edge and 2 mm away from the edge.

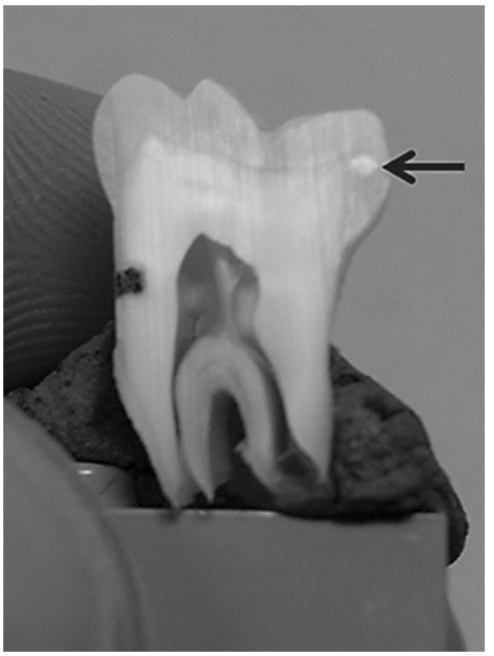

Fig. 8 Vertical wall of one representative sample after 1 day of demineralization on a localized spot. A white spot was created at the top right corner indicated with an arrow.

excitation/probe distances larger than 200 μm away from the edge for both demineralization and remineralization; however, in locations close to the edge (up to ~200 μm), the figures show that LUM signals slightly decrease upon demineralization and slightly increase during the subsequent remineralization. This is consistent with the trends of Fig. 9 and implies that probing closer to the vertical surface which undergoes localized demineralization and remineralization enhances LUM and PTR sensitivity to these processes. However, PTR sensitivity to local conditions on the upper (scanned outer enamel) surface may control the relative signals at the scanned locations. All PTR frequency scans of Fig. 11 converge above 100 Hz, i.e., they become less sensitive or outright insensitive to the condition of the vertical wall, as expected when the decreasing thermal diffusion length [computed as 37.6 μm at 100 Hz using Eq. (1) and thermal diffusivity of enamel $\alpha_E = 4.445\times 10^{-7}$ m^2/s (Refs. 24 and 25)] does not reach the vertical wall (thermally thick condition) to undergo wall-condition-dependent confinement for each probe location indicated in the figures.

Furthermore, there were no expected significant contribution changes to the PTR signal from vertical wall back-scattering during localized demineralization, as the large majority of wall sites remained unaltered. This is unlike the full-wall

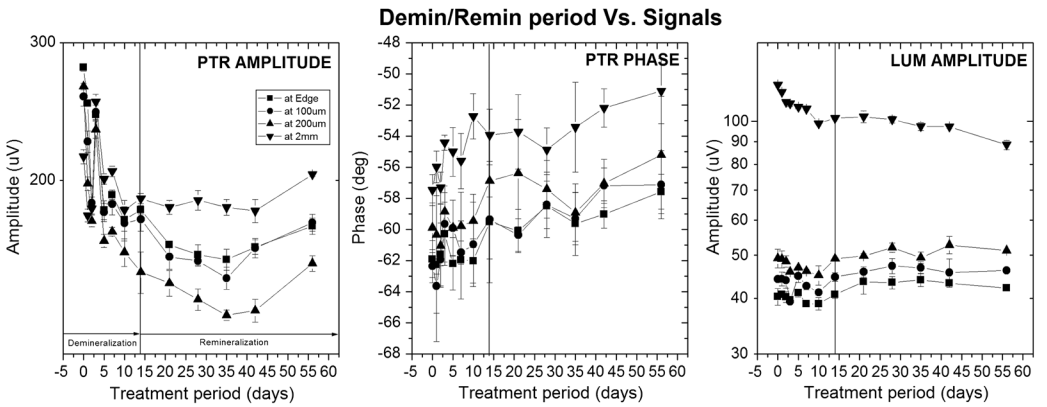

Fig. 9 PTR-LUM scans at fixed positions after each period of demineralization and remineralization of the localized spot. Demineralization occurred from day 1 to 14; remineralization occurred from day 15 to day 56.

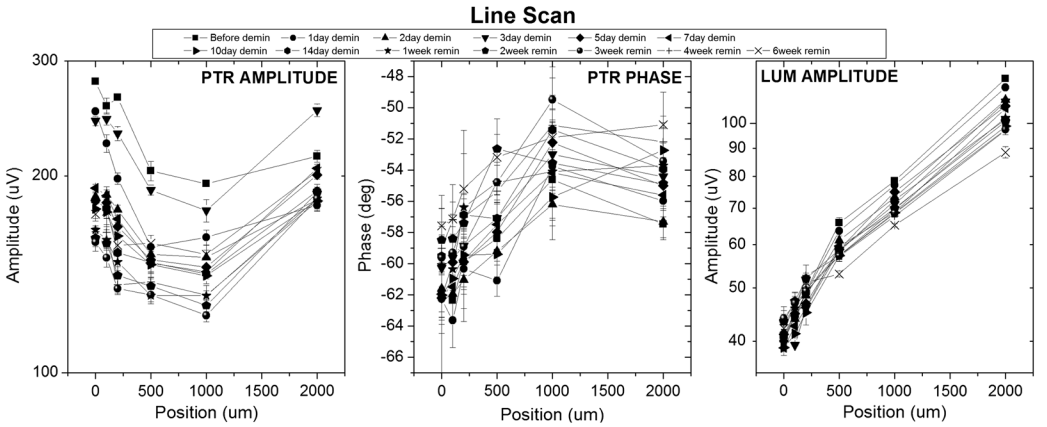

Fig. 10 Line scan data obtained after each period of demineralization and remineralization of the localized spot. PTR signals were obtained at 2 Hz and LUM signals were obtained at 200 Hz.

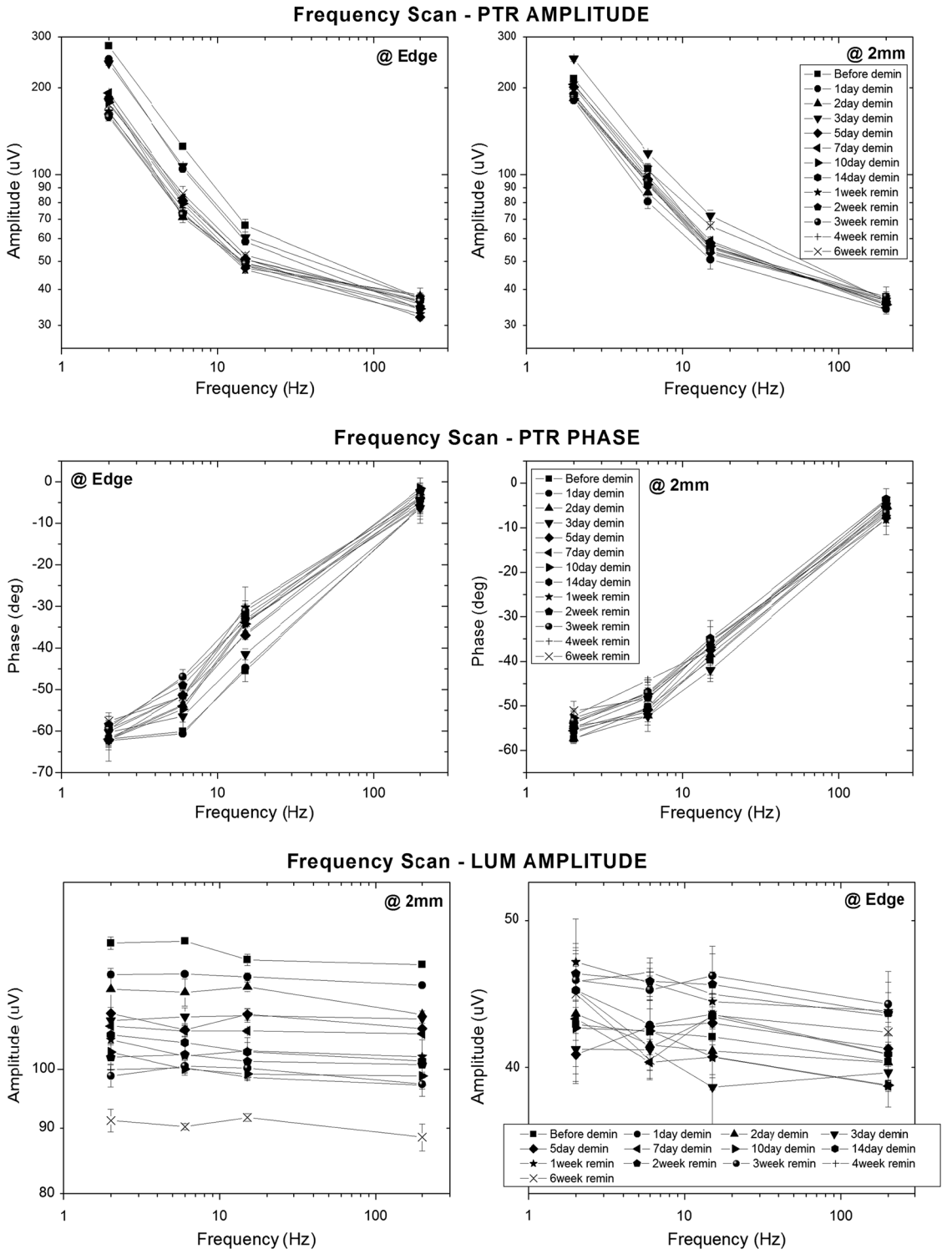

Fig. 11 Frequency scan PTR amplitude, PTR phase, and LUM amplitude data obtained after each period of demineralization and remineralization of the localized spot. Measurements were taken at different locations on the side surface of tooth: at the edge and 2 mm away from the edge.

demineralization process which was seen to affect the PTR signal as far away as 2 mm from the wall (Fig. 6).

4 Conclusions

It was demonstrated that the PTR-LUM system is sensitive to different demineralization and remineralization conditions on the vertical wall of sectioned teeth. Various gap sizes between the composite restoration block and the tooth sample and different types of optical quality materials placed against the vertical wall of the tooth sample resulted in different optothermal properties of the vertical wall and hence in changes of PTR-LUM signals. In those experiments LUM amplitude was found to be more sensitive than PTR to the type of restoration or other materials with different optical properties placed in lieu

of the restoration. The conclusion here is that back-scattered light from particular materials (including composite resin restoration materials) depends on the nature and surface structure of the material and contributes to backward passage through the adjacent vertical enamel wall, thereby enhancing the effect of wall demineralization and the PTR-LUM signal sensitivity to the degree and geometry of demineralization. It was found that this back-passage mechanism when combined with the forward transmission of light through the wall is able to detect the presence and degree of vertical wall demineralization (full or spot). Changes in PTR amplitude and phase signals could be observed with increasing demineralization in both line and frequency scans. Correspondingly, LUM signal amplitudes decreased with days of demineralization in both line and frequency scans. However, the amount of changes of PTR amplitude after each demineralization was larger than that of LUM amplitude. This may indicate that PTR is more sensitive to demineralization than LUM. PTR amplitudes exhibited a correlation coefficient of 0.941 with mineral loss in the statistical analysis. LUM amplitude signals exhibited a correlation coefficient of −0.998 with lesion depth. These results show that demineralization affected both PTR and LUM signal behavior of each sample and these methods can be used simultaneously, in turn, to monitor caries development on the vertical wall adjacent to a restoration composite material.

Investigation of the effects on PTR-LUM of the more clinically relevant case of localized demineralization and remineralization demonstrated that PTR-LUM has the ability to detect demineralization and remineralization localized at a small area (spot) of the vertical enamel wall of the sectioned tooth. The PTR signal amplitudes decreased upon demineralization and increased upon remineralization; the PTR phases increased with both demineralization and remineralization; and LUM signal amplitudes decreased with demineralization while exhibiting enhanced sensitivity to remineralization at probe locations close to the vertical wall. These results are also consistent with the findings of the entire-wall demineralization study. The line scan results of this study regarding PTR-LUM sensitivity to artificial demineralization lesions on vertical walls are further supported by clinical results on patients with secondary caries adjacent to restorations using a dental clinic version of the PTR-LUM technique capable of monitoring early demineralization caries in human teeth.[26]

Acknowledgments

This work was supported by The Health Technology Exchange (HTX) and the 2007 (Inaugural) Ontario Premier's Award in Science and Technology to AM.

Disclosures: Dr. Stephen Abrams and Dr. Andreas Mandelis are co-founders of Quantum Dental Technologies, the company that has developed and is marketing The Canary System. Jungho Kim, Jaclyn Vu, and Bennett Amaechi have no conflicts of interest to report.

References

1. I. A. Mjör and F. Toffenetti, "Secondary caries: a literature review with case reports," *Quintessence Int.* **31**(3), 165–179 (2000).
2. E. A. Kidd, "Diagnosis of secondary caries," *J. Dent. Educ.* **65**(10), 997–1000 (2001).
3. E. Hals and I. Kvinnsland, "Structure of experimental *in vitro* and *in vivo* lesions around composite [Addent XV] fillings," *Scand. J. Dent. Res.* **82**(7), 517–526 (1974).
4. E. A. M. Kidd, "Microleakage: a review," *J. Dent.* **4**(5), 199–206 (1976).
5. P. Dionysopoulos, N. Kotsanos, and Y. Papadogianis, "Secondary caries formation *in vitro* around glass ionomer-lined amalgam and composite restorations," *J. Oral Rehabil.* **23**(8), 511–519 (1996).
6. K. D. Jorgensen and S. Wakumoto, "Occlusal amalgam fillings: marginal defects and secondary caries," *OdontolTidskr.* **76**(1), 43–54 (1968).
7. E. A. Kidd, S. Joyston-Bechal, and D. Beighton, "Marginal ditching and staining as a predictor of secondary caries around amalgam restorations: a clinical and microbiological study," *J. Dent. Res.* **74**(5), 1206–1211 (1995).
8. L. Özer, "The relationship between gap size, microbial accumulation and the structural features of natural caries in extracted teeth with class II amalgam restorations," MS Thesis, University of Copenhagen (1997).
9. P. Totiam et al., "A new *in vitro* model to study the relationship of gap size and secondary caries," *Caries Res.* **41**(6), 467–473 (2007).
10. H. M. Nassar and C. González-Cabezas, "Effect of gap geometry on secondary caries wall lesion development," *Caries Res.* **45**(4), 346–352 (2011).
11. L. A. F. Pimenta, M. F. d. L. Navarro, and A. Consolaro, "Secondary caries around amalgam restorations," *J. Prosthet. Dent.* **74**(3), 219–222 (1995).
12. E. A. M. Kidd and D. Beighton, "Prediction of secondary caries around tooth-colored restorations: a clinical and microbiological study," *J. Dent. Res.* **75**(12), 1942–1946 (1996).
13. P. A. Mileman and W. B. van den Hout, "Comparing the accuracy of Dutch dentists and dental students in the radiographic diagnosis of dental caries," *Dentomaxillofac. Radiol.* **31**(1), 7–14 (2002).
14. A. Zoellner et al., "Histologic and radiographic assessment of caries-like lesions localized at the crown margin," *J. Prosthet. Dent.* **88**(1), 54–59 (2002).
15. A. Zoellner et al., "Secondary caries in crowned teeth: correlation of clinical and radiographic findings," *J. Prosthet. Dent.* **88**(3), 314–319 (2002).
16. J. Bader, "Clinical examination alone detects more secondary caries on crowned teeth than radiograph alone," *J. Evid. Base Dent. Pract.* **3**(2), 90–91 (2003).
17. R. J. Jeon et al., "Diagnosis of pit and fissure caries using frequency-domain infrared photothermal radiometry and modulated laser luminescence," *Caries Res.* **38**(6), 497–513 (2004).
18. R. J. Jeon et al., "Nonintrusive, noncontacting frequency-domain photothermal radiometry and luminescence depth profilometry of carious and artificial subsurface lesions in human teeth," *J. Biomed. Opt.* **9**(4), 804–819 (2004).
19. R. J. Jeon et al., "*In vitro* detection and quantification of enamel and root caries using infrared photothermal radiometry and modulated luminescence," *J. Biomed. Opt.* **13**(3), 034025 (2008).
20. S. Al-Khateeb et al., "Light-induced fluorescence studies on dehydration of incipient enamel lesions," *Caries Res.* **36**(1), 25–30 (2002).
21. E. de Josselin de Jong, A. H. I. M. van der Linden, and J. J. ten Bosch, "Longitudinal microradiography: a non-destructive automated quantitative method to follow mineral changes in mineralised tissue slices," *Phys. Med. Biol.* **32**(10), 1209–1220 (1987).
22. G. J. Christensen, "Marginal fit of gold inlay castings," *J. Prosthet. Dent.* **16**(2), 297–305 (1966).
23. J. W. McLean and J. A. Von Fraunhofer, "The estimation of cement film thickness by an *in vivo* technique," *Br. Dent. J.* **131**(3), 107–111 (1971).
24. M. Braden, "Heat conduction in normal human teeth," *Arch. Oral Biol.* **9**(4), 479–486 (1964).
25. W. S. Browns, W. A. Dewey, and H. R. Jacobs, "Thermal properties of teeth," *J. Dent. Res.* **49**(4), 752–755 (1970).
26. Quantum Dental Technologies, "The Canary System," http://www.thecanarysystem.com (1 May 2012).